

THEORETICAL APPROACH TO LABYRINTH SEAL FORCES - CROSS-COUPLED STIFFNESS OF A STRAIGHT-THROUGH LABYRINTH SEAL

Toshio Kameoka, Toru Abe, and Takeshi Fujikawa
Kobe Steel Ltd.
Kobe, Japan

Considering that there are two kinds of three dimensional flows in a labyrinth seal, a jet flow and a core flow, theoretical equations are set up concerning the motion of each flow. The pressure distribution within the labyrinth is calculated, when the rotor shaft makes a small displacement from the center line of the casing, keeping parallel with it.

The theoretical values of cross coupled stiffness obtained by integrating the pressure under different labyrinth geometries and operating conditions through these formulas are compared with the experimental data presented by other researchers. The theoretical and experimental results show a satisfactory agreement.

1. INTRODUCTION

A self-excited rotor whirl sometimes occurs in high speed, high pressure turbo-machinery, and it is argued that one of the causes of the vibration is due to the labyrinth seal force. Recently, carefully prepared and precisely measured experiments have been carried out, which make possible a fairly exact prediction of the labyrinth seal forces. However, the scope of validation of the prediction should be within the range of reference of the experiments, because of the complexity of the phenomena, unless theoretical formulas verified with experimental data are available. In reality, commercial turbo-machines are normally furnished with labyrinth seals having a number of mixing chambers and are operated under much higher pressure than in experiments.

This paper proposes a method of calculating the asymmetrical pressure distribution in a labyrinth seal caused by the parallel displacement of the shaft, introducing a new mathematical model suggesting that there exist two kinds of independent three dimensional flows, interacting with each other, and that the circumferential variation of static pressure in the mixing chamber comes from the lack of uniformity of the circumferential velocity of the core flow, which is partly originated from the spiral flow effect of the jet flow.

2. NOTATION

$a_0, b_0, c_0, d_1, d_2, d_3, e_0$ = factors relating to fluid friction

$c, (m/s)$ = circumferential velocity of core flow
 $f, f_m, (m^2)$ = cross sectional area of mixing chamber and that of core flow, respectively
 $f_s, (m^2)$ = cross sectional area of jet flow on the meridian plane between successive seal strips
 $N, (-)$ = number of mixing chamber
 $n, (m^{-1})$ = convergency of seal clearance
 $p, (P_a)$ = pressure
 $p_o, (P_a)$ = inlet pressure
 $q, (kg/m \cdot s)$ = mass flow of leakage per unit time per unit circumferential length
 $q_o, (kg/m \cdot s)$ = ditto, under concentric position of rotor
 $R, (J/kg \cdot K)$ = gas constant
 $R_o, (m)$ = inner radius of casing
 $r, (m)$ = radius of rotor
 $s, (m)$ = pitch of seal strips
 $s_o, (m)$ = wetted perimeter of core flow
 $T, (K)$ = gas temperature
 $u, (m/s)$ = circumferential velocity of jet flow
 $u_o, (m/s)$ = tangential velocity of entry swirl
 $u_r, (m/s)$ = circumferential velocity of rotor
 $\alpha, (-)$ = factor of contraction of flow
 $\beta, (-)$ = pressure ratio, exit to inlet
 $\delta, (m)$ = tip clearance of seal strips
 $\delta_o, (m)$ = ditto, in the middle of labyrinth
 $\theta, (rad)$ = helical angle of jet flow
 $\theta_o, (rad)$ = angle of expansion of jet flow in meridian plane
 $\lambda_1, \lambda_2, \lambda_{12}, \lambda_3, (-)$ = coefficients of fluid friction in circumferential direction for $\tau_1, \tau_2, \tau_{12}, \tau_3$, respectively
 $\mu, (P_a \cdot s)$ = viscosity of gas
 $\nu_{i-1,1}, (-)$ = coefficient of carry over from (i-1)-th to i-th chamber
 $\rho, (kg/m^3)$ = density of gas
 $\tau_1, \tau_2, \tau_{12}, \tau_3, (P_a)$ = circumferential component of shear stress due to fluid friction between jet flow and casing wall, between the core flow and the rotor, between the jet flow and the core flow, and between the jet flow and the seal strip, respectively
 Subscript, Superscript
 i = quantity at the i-th chamber in the direction φ
 $i-1, i$ = quantity at the boundary between (i-1)-th and i-th chamber in the direction φ
 \wedge = quantity under concentric position of rotor

3. FLOW OF GAS IN A LABYRINTH

3.1 Jet flow and core flow

It has been known for many years that the meridian flow in a labyrinth is somewhat similar to the flow illustrated in Fig. 1. The flow of gas which has passed through the tip clearance of the seal strip, here called a jet flow, expands and increases its width when it goes through the mixing chamber. This flow also has a circumferential velocity due to the entry swirl and the peripheral velocity of the rotor. Thus, gas particles in this flow move

downwards along a helical stream line, illustrated in Fig. 2. On the other hand, the gas flow in the mixing chamber, here called a core flow, forms a vortex within the surrounding walls on a meridian plane. This core flow also moves in a circumferential direction induced by the tangential speed of the rotor, and consequently the particles in this flow move along a helical stream line in the mixing chamber, as illustrated in Fig. 2.

3.2 Assumptions on the flow

The following assumptions are used to analyze the three dimensional flows:

- (a) Fluid which flows in the labyrinth is an ideal gas.
- (b) Since the change in temperature caused by a change of pressure is neutralized immediately, the temperature in the labyrinth is constant.
- (c) The static pressure is constant on a meridian plane in a mixing chamber.
- (d) The coefficient of "carry over", the coefficient of fluid friction and the wetted perimeter of the channel when the rotor is in a eccentric position, are to be the same value as those under the concentric position of the rotor.
- (e) Pressure difference between two adjoining points partitioned with a seal strip is small.
- (f) The boundary of the jet flow in a chamber on a meridian plane is a tangent to the outer edge of the throat.
- (g) Interchanging of fluid mass takes place between the jet flow and the core flow.
- (h) The circumferential component of the core flow velocity is constant on a meridian plane in a chamber.
- (i) Even in the eccentric position of the rotor, the influence of the eccentricity on the jet flow velocity is small enough for its variation to be neglected.

3.3 Fluid friction acting at the boundary of the flow

The shearing stress τ , due to fluid friction, acting at the boundary of a turbulent flow which flows in a narrow gap between two parallel planes can be expressed by the formula,

$$\tau = \frac{1}{4} \lambda \rho V^2, \quad \lambda = 0.133 \text{ Re}^{-1/4}$$

Where V is the mean velocity of the flow, and Re is Reynold's number relating to the distance of the planes.

In order to estimate the force acting between the flows in a labyrinth the above relationship is applied to the flows. Here, since, the movement of fluid particles in both the jet and the core flow in a circumferential direction is mainly discussed, it becomes necessary to know the relationship between the shearing stress and the velocity, both in a circumferential direction. This relationship can be obtained by considering the relation between the circumferential flow velocity and the circumferential component of shearing stress acting in the direction of absolute velocity. Thus, in case of a labyrinth with rotating seal strips and of the conditions, $u < u_r$ the shearing stress τ_1, τ_2 and τ_3 acting between the jet flow and the casing wall, between the core flow and the channel wall, and between the jet flow and the seal strip, respectively relating to the circumferential direction, can be expressed as follows:

$$\tau_1 = \frac{1}{4} \rho \lambda_1 u^2, \quad \lambda_1 = 0.133 (1 + (v/u)^2)^{\frac{3}{8}} (a_0 q_0 u / (\mu v))^{-\frac{1}{4}} \quad (1)$$

$$\tau_2 = \frac{1}{4} \rho \lambda_2 (u_r - c)^2, \quad \lambda_2 = 0.133 (1 + (b_0 v)^2 / (u_r - c)^2)^{\frac{3}{8}} ((u_r - c) c_0 f_m \rho / (s_0 \mu))^{-\frac{1}{4}} \quad (2)$$

$$\tau_3 = \frac{1}{4} \rho \lambda_3 (u_r - u)^2, \quad \lambda_3 = d_3 \lambda_1 \quad (2')$$

By a similar principle, the shearing stress acting at the boundary between the jet flow and the core flow in a circumferential direction leadsto the following equation.

$$\tau_{12} = \frac{1}{4} \rho \lambda_{12} (c - u)^2, \quad \lambda_{12} = d_1 d_2 \lambda_1 \lambda_2 (\sqrt{\lambda_1 d_1} + \sqrt{\lambda_2 d_2})^{-2} \sqrt{1 + (1 - e_0)^2 v^2 / (u - c)^2} \quad (3)$$

4. FUNDAMENTAL EQUATIONS OF THE FLOW IN A LABYRINTH

4.1 Equations at the eccentric position of the rotor

By the small displacement x, y of the rotating shaft, as shown in Fig. 3, a small variation in static pressure will be added to the pressure distribution of the concentric labyrinth. When the seal strips are mounted on the rotor and the circumferential velocity of the jet flow is smaller than the peripheral velocity of the rotor, the fundamental equations dominating the flows are derived in the following way in order to calculate such a variation in pressure.

(1) Seal clearance

From the geometrical configuration, comes the equation,

$$\delta_{i-1,i} = \delta_0 (1 - ns(2i - N - 2)/2) - x \cos \varphi - y \sin \varphi \quad (4)$$

(2) Mass flow of gas leaking through the seal clearance

Instead of neglecting the approaching speed of gas to the throat, the effects of "carry over" of the labyrinth seal is introduced. Thermodynamic relations provide:

$$q_{i-1,i}^2 = \delta_{i-1,i}^2 a_{i-1,i}^2 (p_{i-1}^2 - p_i^2) / (RT) \quad (5)$$

(3) The equation of continuity

The stream lines of the jet flow in a mixing chamber are approximately represented by straight lines having gradient of $\hat{\theta}_1$, as shown in Fig. 4(a). A and B is the inlet and the outlet of a stream tube having a small circumferential length $r d\varphi$ at the center of the mixing chamber, and q_A and q_B represent the mass flow rate at A and B, respectively. Due to the difference in the mass flow rate $q_A - q_B$ the mass in the stream tube segment AB is increased by $(q_A - q_B) \cdot r d\varphi dt$ in the duration of time dt . A part of the above increase in gas increases its own density and the rest of the quantity, q_{s1} moves to the core flow just beneath the stream tube, so that

$$q_{s1} = (q_{i-1,i} - q_{i,i+1}) - \frac{s}{2r} \tan \hat{\theta}_1 \frac{\partial}{\partial \varphi} (q_{i-1,i} + q_{i,i+1}) - \frac{\partial(\rho_1 f_{s1})}{\partial t}$$

On the other hand, as illustrated in Fig. 4 (b), the core flow segment which exists between D and E at the time t is to be shifted circumferentially to the position between D' and E' at the time $t + dt$.

Since the increase of mass in the volume element D'E' against that in the volume element DE is equal to the quantity of gas having come from the jet flow, the equation for the conservation of mass in a circumferential direction

provides the following equation of continuity.

$$r \frac{\partial(p_1 f_1)}{\partial t} + \frac{\partial(f_{m1} p_1 c_1)}{\partial \varphi} + RT \left(r(q_{1,i+1} - q_{1-i,1}) + \frac{s}{2} \tan \hat{\theta}_1 \frac{\partial}{\partial \varphi} (q_{1-i,1} + q_{1,i+1}) \right) = 0 \quad (6)$$

(4) The equation for the conservation of momentum of the core flow in a circumferential direction

As the increase of momentum in a circumferential direction in the volume element D'E' against that in the volume element DE, shown in Fig. 4 (b), consists of the increase in the circumferential momentum of the gas coming from the jet flow, of that due to the pressure gradient and the increase of the cross-sectional area of the core flow, and of that due to the fluid friction, the following equation can be obtained.

$$\left[\frac{c-u}{pf_m} \right]_1 \frac{\partial(pf_m)_1}{\partial t} + \frac{\partial c_1}{\partial t} + \left[\frac{(c-u)c}{pf_{mr}} \right]_1 \frac{\partial(pf_m)_1}{\partial \varphi} + \frac{(2c-u)_1}{r} \frac{\partial c_1}{\partial \varphi} + \frac{RT}{p_1 r} \frac{\partial p_1}{\partial \varphi} + \left[\kappa' (c-u)^2 - \kappa'' (u_r - c)^2 \right]_1 = 0 \quad (7)$$

where $\kappa' = \lambda_{12} s / 4 f_m$, $\kappa'' = \lambda_2 s_0 / 4 f_m$

4.2 Relationships when the shaft is at the center line of the casing

(1) Coefficient of "carry over" in a straight-through labyrinth

The following equation, which is a slightly modified version of Komotori's equation(ref.1) is used.

$$\hat{\nu}_{1-i,1} = \left[1 - \left(\frac{\hat{\delta}_{1-i,1}}{\hat{\delta}_{1-2,1-i}} \right)^2 \frac{\hat{\rho}_1}{\hat{\rho}_{1-i}} \hat{A}_{1-i} (2 - \hat{A}_{1-i}) \right]^{-\frac{1}{2}}, \quad \hat{A}_{1-i} = \frac{\hat{\delta}_{1-2,1-i} \cdot \alpha}{\hat{\delta}_{1-2,1-i} \cdot \alpha + s \tan \theta_0} \quad (8)$$

(2) Equation of conservation of momentum for the jet flow

As already mentioned, it is assumed in this case that so that the positive direction of $\tau_1, \tau_2, \tau_{12}, \tau_3$ should be determined, $\hat{u}_1 < c_1 < u_r$

τ_1 : in such a direction that the jet flow is decelerated

τ_2 : " " " the core flow is accelerated

τ_{12} : " " " the jet flow is accelerated by the core flow

τ_3 : " " " the jet flow is accelerated.

In the stream tube segment AB, illustrated in Fig. 5, the increase in the momentum of the gas in a circumferential direction in the volume element A'B' against AB in a small duration of time dt should be equal to the sum of the momentum added to this stream tube segment by the (i-1)-th and i-th and core flow in a circumferential direction. Thus, the following equation is obtained.

$$(\hat{u}_1 - \hat{u}_{1-i}) q_0 dt = \frac{1}{2} \left(-\hat{\tau}_{1,i-1} + \hat{\tau}_{12,i-1} + \hat{\tau}_{3,i-1} \tan \theta_0 \right) s dt + \frac{1}{2} \left(-\hat{\tau}_{1,i} + \hat{\tau}_{12,i} + \hat{\tau}_{3,i} \tan \theta_0 \right) s dt \quad (9)$$

(3) Fundamental equations when the rotor is in a concentric position

Substituting $x=y=0$ and $\partial/\partial t = \partial/\partial \varphi = 0$ for the fundamental equations, give

$$\hat{\delta}_{1-i,1} = \delta_0 \left[1 - \frac{s s}{2} (2i - N - 2) \right] \quad (10)$$

$$q_0^2 = (\alpha \cdot \hat{\delta}_{1-i,1} \cdot \hat{\nu}_{1-i,1})^2 (\hat{p}_{i-1}^2 - \hat{p}_1^2) / RT \quad (11)$$

$$\hat{\kappa}_1 (\hat{c}_1 - \hat{u}_1) - \hat{\kappa}_1 (u_r - \hat{c}_1)^2 = 0 \quad (12)$$

5. SOLUTION OF THE EQUATIONS

5.1 Mass flow rate, pressure, and circumferential velocity of flow at the concentric position of the rotor

These parameters can be calculated in the following way.

- (a) Values of \hat{p}_1 and \hat{q}_0

From eqs. (8), (10) and (11), q_0 can be written as follows:

$$\hat{q}_0 = \frac{\hat{p}_0 - \hat{p}_{N+1}}{\sum_{i=1}^{N+1} \hat{B}_i}$$

$$\hat{B}_i = \frac{RT}{(\alpha \delta_0)^2} \left[\left\{ 1 - \frac{sn}{2} (2i - N - 2) \right\}^{-2} - \frac{\hat{\rho}_i}{\hat{\rho}_{i-1}} \left\{ 1 - \frac{sn}{2} (2i - N - 4) \right\}^{-2} \hat{A}_{i-1} (2 - \hat{A}_{i-1}) \right] \quad (13)$$

Using the pressure at the inlet $\hat{p}_0 = \hat{p}_0$, and at the outlet $\hat{p}_{N+1} = \beta p_0$, values of q_0 and $\hat{p}_1 \sim \hat{p}_N$ can be obtained with the necessary accuracy from the above equation through iterative calculation.

- (b) Values of \hat{u}_1 and \hat{c}_1

From eq. (12)

$$\hat{c}_1 = \hat{A}_{2,1} u_r + \hat{A}_{1,1} \hat{u}_1 \quad (14)$$

and, from eq. (14) and eq. (9) substituted by eqs. (1)-(3)

$$\left[\frac{\hat{s} p_i (\hat{\lambda}_{1,i} - \hat{E}_i)}{8RT} \right] \hat{u}_i^2 + \left[q_0 + \frac{\hat{s} p_i \hat{E}_i u_r}{4RT} \right] \hat{u}_i + \left[\frac{\hat{s} p_{i-1} (\hat{\lambda}_{1,i-1} - \hat{E}_{i-1}) \hat{u}_{i-1}^2}{8RT} \right. \\ \left. + \left(-q_0 + \frac{\hat{s} p_{i-1} \hat{E}_{i-1} \cdot u_r}{4RT} \right) \hat{u}_{i-1} - \frac{\hat{s} u_r^2 (\hat{p}_i \hat{E}_i + \hat{p}_{i-1} \cdot \hat{E}_{i-1})}{8RT} \right] = 0 \quad (15)$$

are derived, where

$$\hat{E}_i = \hat{\lambda}_{12,i} (\hat{A}_{2,i})^2 + d_3 \hat{\lambda}_{1,i} \tan \theta_0, \quad \hat{A}_{2,i} = 1 - \hat{A}_{1,i}$$

$$\hat{A}_{1,i} = \frac{K \sqrt{s/s_0}}{1 + \sqrt{\hat{\lambda}_{2,i} / \hat{\lambda}_{1,i}} + K \sqrt{s/s_0}} \quad K = \left[1 + \left\{ \frac{(1 - e_0) \hat{v}_1}{\hat{u}_1 - \hat{c}_1} \right\}^2 \right]^{\frac{1}{4}}$$

For the given value of parameters at the $(i-1)$ -th chamber, \hat{u}_1 can be obtained by solving the quadratic equation (15) for \hat{u}_1 . However, the values $\hat{\lambda}_{11}$ and $\hat{\lambda}_{121}$ which appear in the coefficient of that equation, are unfortunately a complicated function of \hat{u}_1 , so that \hat{u}_1 can be obtained from that equation by applying an iterative calculation for each chamber.

5.2 Pressure distribution when the rotor is located in the eccentric position

The variation of p , c and q due to a small amount of displacement of the rotating shaft, must be small compared with those values at the concentric position of the rotor. Further, each increment of p , c and q must be a periodic function of φ , so that the increment can be expanded by Fourier series. Taking the terms of lowest order of the series, the solution of the fundamental equations (5), (6), (7) can be simply put as follows.

$$\begin{aligned}
p_1 &= \hat{p}_1 + p_0 \{ a_1 \cos \varphi + b_1 \sin \varphi \} \\
c_1 &= \hat{c}_1 + u_r \{ d_1 \cos \varphi + e_1 \sin \varphi \} \\
q_{1-1,1} &= q_0 + q_0 \{ k_{1-1,1} \cos \varphi + l_{1-1,1} \sin \varphi \}
\end{aligned} \tag{6}$$

where unknown parameters a_i, b_i, \dots are the linear function of x, y , and

$$\begin{aligned}
|a_1 \cos \varphi + b_1 \sin \varphi| &\ll \hat{p}_1 / p_0 \\
|d_1 \cos \varphi + e_1 \sin \varphi| &\ll \hat{c}_1 / u_r \\
|k_{1-1,1} \cos \varphi + l_{1-1,1} \sin \varphi| &\ll 1.
\end{aligned} \tag{7}$$

Since the equation obtained by substituting eq. (16) into eq. (5) must hold true for any value of φ , the following equations can be obtained.

$$\begin{aligned}
q_0^2 k_{1-1,1} &= p_0 \hat{D}_{1,1} (\hat{p}_{1-1} a_{1-1} - \hat{p}_1 a_1) - (\hat{p}_{1-1}^2 - \hat{p}_1^2) \hat{D}_{2,1} x \\
q_0^2 l_{1-1,1} &= p_0 \hat{D}_{1,1} (\hat{p}_{1-1} b_{1-1} - \hat{p}_1 b_1) - (\hat{p}_{1-1}^2 - \hat{p}_1^2) \hat{D}_{2,1} y
\end{aligned} \tag{8}$$

As similar equations can be also obtained from eqs. (6) and (7) both substituted by $\varphi = 0$, by eliminating k, l, d, e from these six equations obtained, the following equations result eventually.

$$\begin{aligned}
A_{1,1-1} a_{1-1} + B_{1,1-1} b_{1-1} + A_{1,1} a_1 + B_{1,1} b_1 + A_{1,1+1} a_{1+1} + B_{1,1+1} b_{1+1} &= X_1 \cdot x + Y_1 \cdot y \\
-B_{1,1-1} a_{1-1} + A_{1,1-1} b_{1-1} - B_{1,1} a_1 + A_{1,1} b_1 - B_{1,1+1} a_{1+1} + A_{1,1+1} b_{1+1} &= -Y_1 \cdot x + X_1 \cdot y
\end{aligned} \tag{9}$$

where

$$\begin{aligned}
A_{1,1-1} &= -(1/q_0) RT r p_0 \hat{D}_{1,1} \hat{p}_{1-1} \\
A_{1,1} &= 2 p_0 r \hat{m}_1 \hat{f}_{m,1} [(\hat{c}_1 - \hat{u}_1) \hat{c}_1 + RT] (u_r - \hat{u}_1) / \hat{M}_1 + (1/q_0) RT r p_0 (\hat{D}_{1,1+1} + \hat{D}_{1,1}) \hat{p}_1 \\
A_{1,1+1} &= -(1/q_0) RT r p_0 \hat{D}_{1,1+1} \hat{p}_{1+1} \\
B_{1,1-1} &= RT s p_0 \hat{J}_1 \hat{D}_{1,1} \hat{p}_{1-1} / (2 q_0) \\
B_{1,1} &= -p_0 \hat{f}_{m,1} [(\hat{c}_1 - \hat{u}_1) \hat{c}_1 + RT] (2 \hat{c}_1 - \hat{u}_1) / \hat{M}_1 + RT s p_0 \hat{J}_1 (\hat{D}_{1,1+1} - \hat{D}_{1,1}) \hat{p}_1 / (2 q_0) \\
B_{1,1+1} &= -RT s p_0 \hat{J}_1 \hat{D}_{1,1+1} \hat{p}_{1+1} / (2 q_0) \\
X_1 &= 2(1-\alpha) s r \hat{m}_1 \hat{p}_1 \hat{c}_1 (\hat{c}_1 - \hat{u}_1) (u_r - \hat{u}_1) / \hat{M}_1 \\
&\quad - (1/q_0) RT r [\hat{D}_{2,1} \hat{p}_{1-1}^2 - (\hat{D}_{2,1} + \hat{D}_{2,1+1}) \hat{p}_1^2 + \hat{D}_{2,1+1} \hat{p}_{1+1}^2] \\
Y_1 &= (1-\alpha) s \hat{p}_1 \hat{c}_1 [1 - (\hat{c}_1 - \hat{u}_1) (2 \hat{c}_1 - \hat{u}_1) / \hat{M}_1] \\
&\quad + RT s \hat{J}_1 [\hat{D}_{2,1} \hat{p}_{1-1}^2 + (\hat{D}_{2,1+1} - \hat{D}_{2,1}) \hat{p}_1^2 - \hat{D}_{2,1+1} \hat{p}_{1+1}^2] / (2 q_0) \\
\hat{M}_1 &= [2 r \hat{m}_1 (u_r - \hat{u}_1)]^2 + (2 \hat{c}_1 - \hat{u}_1)^2 \\
\hat{D}_{1,1} &= \alpha^2 \hat{\sigma}_0^2 \hat{\nu}_{1-1,1}^2 \left\{ 1 - \frac{s n}{2} (2i - N - 2) \right\}^2 / (RT) \\
\hat{D}_{2,1} &= \alpha^2 \hat{\sigma}_0^2 \hat{\nu}_{1-1,1}^2 \left\{ 1 - \frac{s n}{2} (2i - N - 2) \right\} / (RT) \\
\hat{f}_{m,1} &= s \left[R_0 - r - \frac{s}{2} \cdot \tan \theta_0 - \alpha \hat{\sigma}_0 \left\{ 1 - \frac{s n}{2} (2i - N - 2) \right\} \right]
\end{aligned}$$

$$\hat{j}_1 = \hat{u}_1 / \hat{v}_1 \quad \hat{m}_1 = \kappa \hat{A}_{2,1} + \kappa' \hat{A}_{1,1}$$

Equations (19) can be written for $i=1$ upto $i=N$, so that the total number of the equation is $2N$. Since $(a_{i-1})_{i=1} = (b_{i-1})_{i=1} = (a_{i+1})_{i=N} = (b_{i+1})_{i=N} = 0$ is evident, the unknown quantities are $a_i \sim a_N$ and $b_i \sim b_N$. And the total number is also $2N$. The solution, a_i and b_i , therefore, can be obtained by solving the simultaneous linear equation (19) considering the following relationship.

$$a_i = \bar{\alpha}_i x - \bar{\beta}_i y, \quad b_i = \bar{\beta}_i x + \bar{\alpha}_i y$$

The static pressure distribution in a labyrinth can be calculated from the eq. (16).

5.3 Cross coupled stiffness

The pressure in the labyrinth, expressed by eq. (16), provides the force F_x and F_y , acting in the negative direction of x and y axis respectively so that

$$F_x = \sum_{i=1}^N s \cdot r \int_0^{2\pi} p_i \cos \varphi d\varphi = \pi s r p_0 \sum_{i=1}^N a_i \quad (20)$$

$$F_y = \sum_{i=1}^N s \cdot r \int_0^{2\pi} p_i \sin \varphi d\varphi = \pi s r p_0 \sum_{i=1}^N b_i$$

The forward tangential force divided by the displacement of the rotating shaft, so called the coefficient of the cross coupled spring constant K_{xy} , can be represented as follows.

$$K_{xy} = -\pi s r p_0 \sum_{i=1}^N \beta_i \quad (21)$$

6. THE FUNDAMENTAL EQUATIONS FOR THE LABYRINTH HAVING DIFFERENT GEOMETRIES OR OPERATING CONDITIONS

The preceding theory refers to the case when the seal strips are mounted on the rotor and when the peripheral velocity of the rotor is larger than the circumferential velocity of the jet flow. If, on the same geometry of the labyrinth, the peripheral velocity of the rotor is smaller than the circumferential velocity of the jet flow, the positive direction of τ_1 and τ_2 should be determined to be in such a direction that the jet flow is decelerated. Similarly, the positive direction of τ_2 should be the direction in which the core flow is decelerated. The equations can be obtained, in this case, by the same procedure as explained in the previous section. Among these equations thus obtained, the following equations are the essentially different as compared with those of the preceding section.

$$\lambda_2 = 0.133 \left[1 + (b_0 v)^2 / (c - u_r)^2 \right]^{\frac{2}{5}} \left[(c - u_r) c_0 f_m \rho / (s_0 \mu) \right]^{-\frac{1}{4}} \quad (2a)$$

$$\left[\frac{s p_1 (\hat{\lambda}_{1,1} + \hat{E}_1)}{8 R T} \right] \hat{u}_1^2 + \left[q_0 \frac{s p_1 \hat{E}_1 u_r}{4 R T} \right] \hat{u}_1 + \left[\frac{s p_{1-1} (\hat{\lambda}_{1,1-1} + \hat{E}_{1-1})}{8 R T} \right] \hat{u}_{1-1}^2$$

$$-\left(q_0 + \frac{s \hat{p}_{1-1} \hat{E}_{1-1} \cdot u_r}{4RT}\right) \hat{u}_{1-1} + \frac{s u_r^2 (\hat{p}_1 \hat{E}_1 + \hat{p}_{1-1} \cdot \hat{E}_{1-1})}{8RT} = 0 \quad (14a)$$

$$\left(\frac{c-u}{pf_m}\right)_1 \frac{\partial(pf_m)_1}{\partial t} + \frac{\partial c_1}{\partial t} + \left(\frac{(c-u)c}{pf_m r}\right)_1 \frac{\partial(pf_m)_1}{\partial \varphi} + \frac{(2c-u)_1}{r} \frac{\partial c_1}{\partial \varphi} + \frac{RT}{p_1 r} \frac{\partial p_1}{\partial \varphi} - \left[\kappa'(u-c)^2 - \kappa'(c-u_r)^2\right]_1 = 0 \quad (7a)$$

For the straight-through labyrinth, in which the seal strips are mounted inside the casing, the equations can also be obtained by modifying the original equations with the same principle.

7. RESULTS OF NUMERICAL CALCULATION AND THE COMPARISON WITH THE EXPERIMENTAL DATA PRESENTED BY OTHER RESEARCHERS

Factors, $a_0, b_0, c_0, d_1, d_2, d_3, e_0$ which are included in eqs.(1)-(3), as well as α and θ_0 included in eq.(8), are to be decided by the observation of the flow in a labyrinth. However, as some of this data was not available, these factors have been tentatively estimated as follows throughout the calculation based on the procedure here explained.

$$a_0 = 1.5 \quad b_0 = 0.5 \quad c_0 = 1.0 \quad d_1 = 1.0 \quad d_2 = 1.0 \quad d_3 = 1.0 \quad e_0 = 0.5$$

Wachter and Benckert(ref.2) have done an experiment of the static characteristics of a labyrinth having different geometries under different operating conditions. Results of numerical calculation in accordance with the procedure explained in this paper have been compared with the results of the above experiments. The results of their experiments shown in Fig.6 and in Fig.7(a) are obtained using a land-and-groove labyrinth, whereas numerical calculation is on a labyrinth which is deemed to be equivalent to this kind of labyrinth and assumed complete mixing of gas in the mixing chamber on making calculation. As to the effect of the peripheral velocity of the rotor on the lateral force excitation constants, as well as the effect of entry swirl on the constants, calculations not only agree with experiments qualitatively, but also fairly good quantitative agreement is seen between the two. The dimensionless lateral force excitation constants \bar{K}_q^* taken on the ordinate of these diagrams, and the relative admission energy E_o^* taken on the abscissa in Fig.7 are the following values respectively.

$$\bar{K}_q^* = \frac{\partial_o K_{xy}}{r s n p_o (1-\beta)} \quad , \quad E_o^* = \frac{u_o^2}{2(1-\beta)RT + (2R_o q_o RT / p_o (R_o^2 - r^2))^2}$$

Wachter and Benckert have done a further experiment using a straight-through labyrinth with seal strips morticed inside the casing, and examined the effect of entry swirl on the lateral force excitation constants. Comparison of experiments and calculations have also been made in this case, and shown in Fig.7(b). A qualitative agreement of the two values is obtained. However, from a view-point of quantity, the calculated values are much smaller in this case.

Also, Jenny(ref.3) has presented his theoretical formulas, which are composed partly by adopting the empirical relation of parameters. Results of calculation on one example of a labyrinth with axial admission using his formula and those by the procedure in this paper are compared and shown in Fig.8. These two calculated values agree very well.

It is said that, when swirl is applied to a rotating labyrinth in an eccentric position, an additional exciting force is generated in it whose intensity depends on the intensity of the swirl. Calculation has been made to see the influence of the swirl on the rotating labyrinth. The results agree with the tendency, as shown in Fig.9.

Kurohashi et al.(ref.4) have done experiment to examine the influence of the divergency of the seal clearance on the exciting force of a straight through labyrinth. The comparison of calculated values with their experimental data is illustrated in Fig.10. With regard to the statical characteristics it is seen in both values that the diverging clearance provides a stabilizing tendency against the forward whirl of the shaft, and the calculated value agrees qualitatively with the experimental value.

9. CONCLUSION

On the assumption that there exist two kinds of three dimensional flow in a labyrinth, a jet and a core flow, an analysis of the behavior of the flow was made, and a method to calculate the statical behavior of a labyrinth seal was shown. The results of calculation on some examples of labyrinths showed a fairly good agreement with results of experiments, and it can be said that this method is useful to predict the destabilizing force, which originates from a labyrinth seal, and acts on the rotating shaft.

REFERENCES

- (1) Komotori, K.: A Consideration on the Labyrinth Packing of Straight Through Type. Trans. Jpn. Soc. Mech. Eng. 23-133(1957), 617
- (2) Wachter, J. and Benckert, H.: Querkräfte aus Spaltdichtungen - Eine mögliche Ursache für die Laufunruhe von Turbomaschinen. Atomkernenergie Bd.32 (1978), 239 (See also NASA CP-2133, 1980, pp. 189-212.)
- (3) Jenny, R.: Labyrinth as a Cause of Self excited Rotor Oscillations in Centrifugal Compressors. Sulzer Tech. Rev. 4(1980), 149
- (4) Kurohashi, M. et al.: Spring and Damping Coefficients of the Labyrinth Seals. Int. Conf. on Vibrations in Rotating Machinery, Cambridge, (1980)

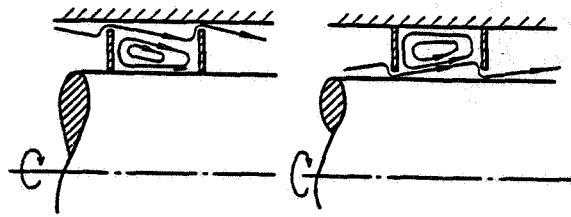


Fig.1 Meridian flow in a straight-through labyrinth seal

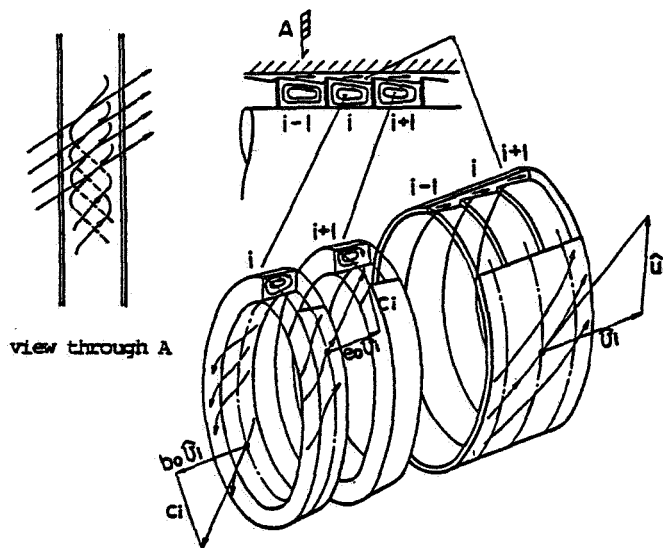


Fig.2 Three dimensional flow in a labyrinth

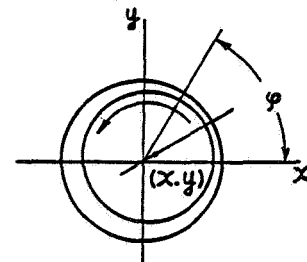


Fig.3 Displacement of rotating shaft

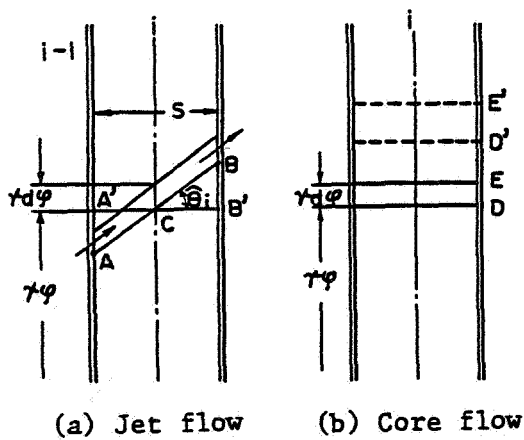


Fig.4 Flow on the development surface

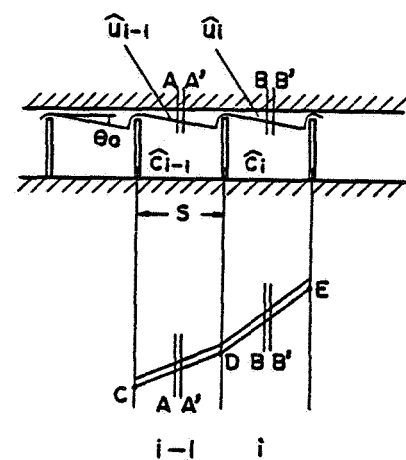


Fig.5 Stream line of jet flow

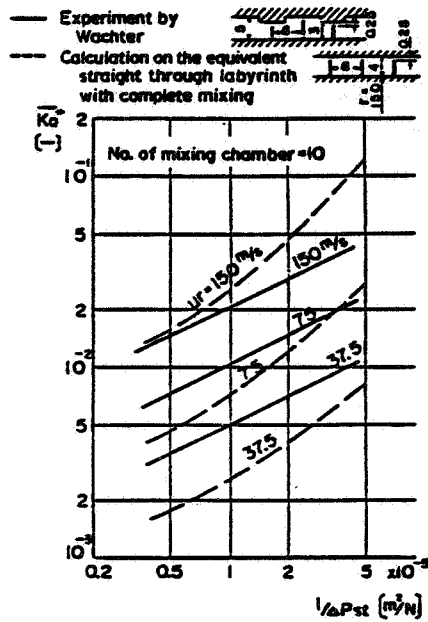


Fig.6 Lateral force spring coefficient

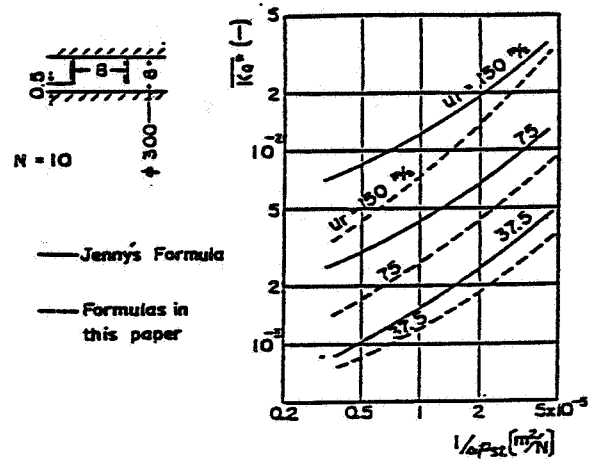
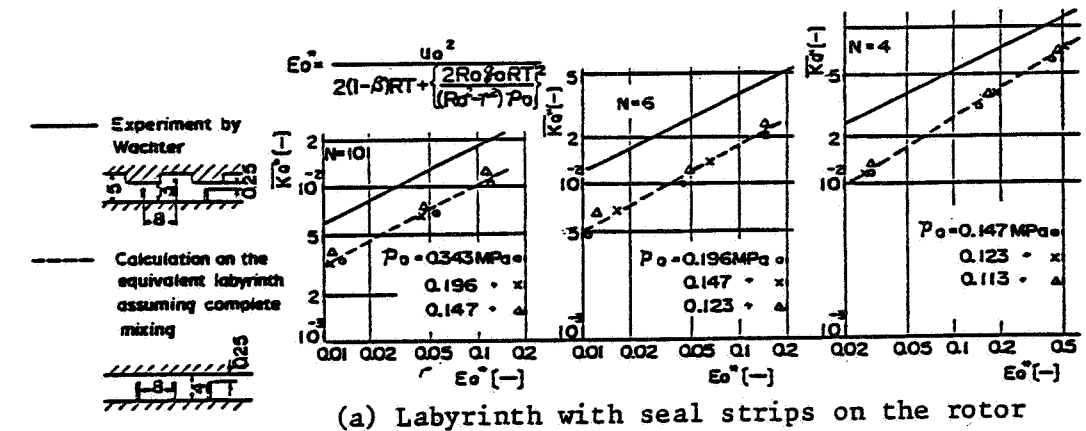
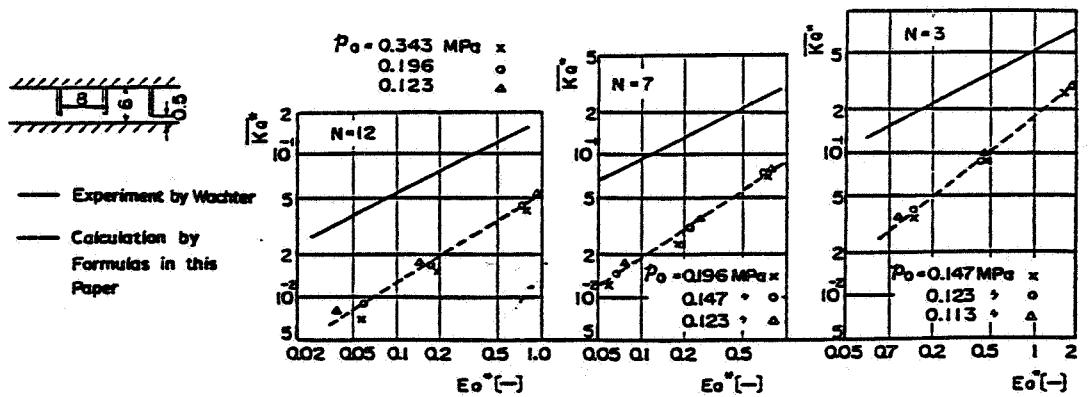


Fig.8 Comparison of lateral force spring coefficient with Jenny's formula



(a) Labyrinth with seal strips on the rotor



(b) Labyrinth with seal strips inside the casing

Fig.7 Lateral force spring coefficient vs relative admission-energy of the flow ($U_r=0$)

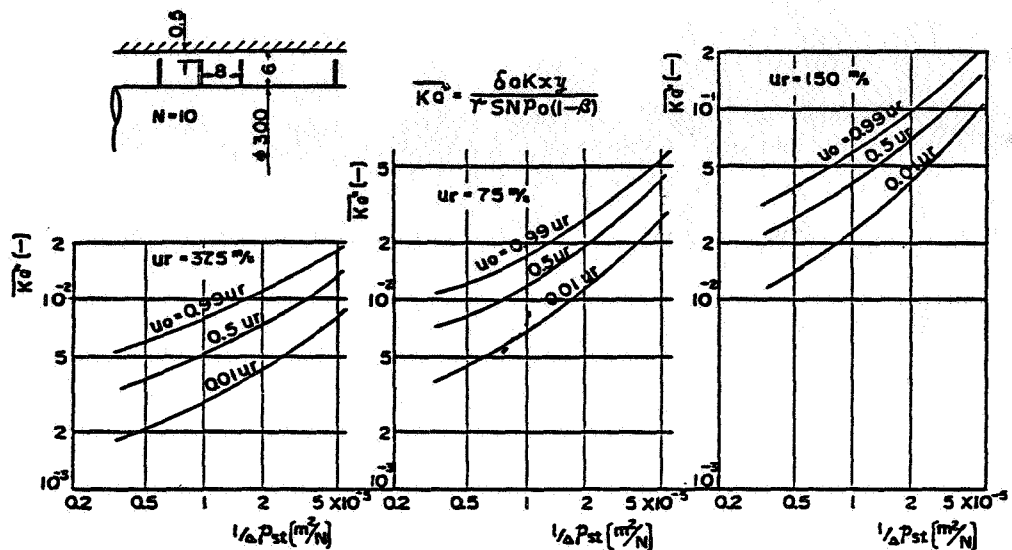
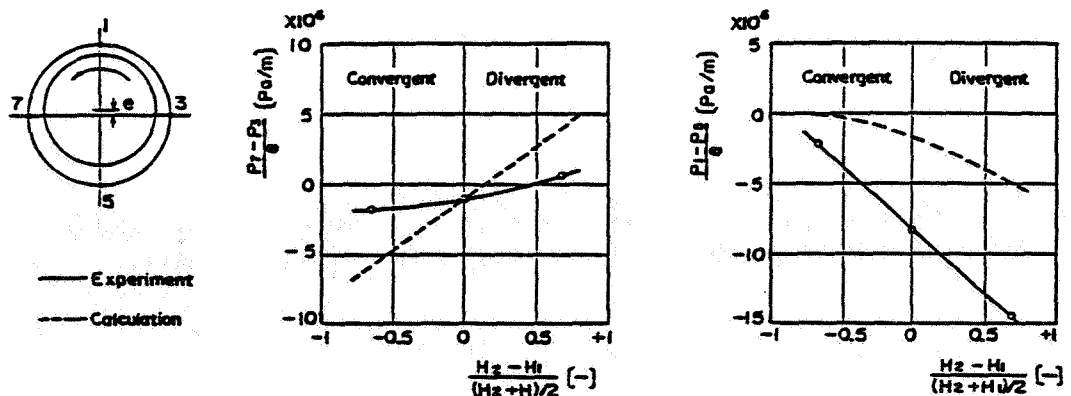


Fig.9 Lateral force spring coefficient of a rotating labyrinth affected by the imposing of entry swirl

| | |
|---|---|
| <p>$D = \frac{H_2 - H_1}{(H_2 + H_1)/2}$</p> <p>Where H_1 = clearance at inlet H_2 = clearance at outlet</p> | <p>No. of mixing chamber: 19</p> <p>Mean clearance: 0.3, 0.4 mm</p> <p>Divergency of clearance, D: -0.667, 0, +0.667</p> <p>Peripheral speed of rotor: 3 ~ 29.4 m/s</p> <p>Kind of gas: air</p> <p>Entry swirl: 0</p> <p>Inlet pressure: 0.3 MPa</p> <p>Outlet pressure: atmospheric</p> <p>Lateral displacement of rotor at inlet: -0.2 ~ +0.2 mm</p> <p>at outlet: -0.2 ~ +0.2 mm</p> |
|---|---|

(a) Parameters of experiment



(b) Comparison of experiments and calculations

Fig.10 Effect of divergency of seal clearance on the pressure distribution in a labyrinth